

# THE CHALLENGES OF CREDIBLE THERMAL PROTECTION SYSTEM RELIABILITY QUANTIFICATION

Lawrence L. Green

NASA Langley Research Center, 1 N. Dryden Street  
M/S 451, Hampton, VA 23681, [lawrence.l.green@nasa.gov](mailto:lawrence.l.green@nasa.gov)

## ABSTRACT

The paper discusses several of the challenges associated with developing a credible reliability estimate for a human-rated crew capsule thermal protection system. The process of developing such a credible estimate is subject to the quantification, modeling and propagation of numerous uncertainties within a probabilistic analysis. The development of specific investment recommendations, to improve the reliability prediction, among various potential testing and programmatic options is then accomplished through Bayesian analysis.

## 1. INTRODUCTION

This paper discusses a Thermal Protection System (TPS) reliability estimation process. The process utilizes a predictive, probabilistic, physics-based TPS model, with uncertainty models informed by various contributors, including material properties data and arc jet test data. The reliability estimation process considers a single TPS failure mode, the bondline over-temperature mode, in which the temperature at the junction between the TPS material and the underlying composite carrier structure is constrained by the carrier structure inter-laminar strength requirement. It is a notable achievement just to enable quantification of the TPS reliability, but the study has moved well beyond that accomplishment to identifying and quantifying specific uncertainty sources that contribute, quantifying the response sensitivities to the mean value and dispersion of those uncertainties, and even to making specific investment recommendations to improve upon the estimated reliability.

There are many challenges associated with developing a credible TPS reliability estimate [1 through 6]. In this context, the term challenge has several meanings: 1) identification of the many relevant uncertainties, 2) credible quantification of those uncertainties, and 3) issues associated with uncertainty reduction and mitigation.

Ten of these challenges are enumerated below and discussed subsequently.

1. Arc Jet Testing
2. Generic Measured Data Issues
3. Material Property Effects / Correlations
4. Trajectory / Orientation
5. Flow Transition
6. Ground-to-Flight Uncertainty
7. Failure Mode Form
8. Reliability Assessment
9. Reliability Cascade
10. Cost / Benefit Modeling

The reliability assessment process, as shown in Fig. 1, is actually the third phase in a TPS synthesis and modeling process, all of which depends upon measured data from numerous sources, and expert opinion, throughout. Color coding has been used in Figs. 1 through 4: yellow for uncertainty sources, cyan for generic process steps, and green for deliverable products.

Details of each of these three phases are illustrated in Figs. 2 through 4 and described subsequently. As shown in Fig. 2, the code development process synthesizes material property data, ablation physics data and Subject Matter Expert (SME) opinion and results in a fixed, configuration-controlled, ablation code version. This fixed code version includes embedded code development uncertainties such as measured data issues and physics approximations. Some of the measured data issues will be described subsequently.

As shown in Fig. 3, the code execution process synthesizes one or more vehicle trajectory, orientation, aerothermal margining assumption and material property specifications and the embedded code development uncertainties (noted above) to yield reliability case results, which should also be subject to configuration control measures. Each of the specifications in this process is a synthesis of data and SME opinion-based. Additionally, each of the

reliability case results includes embedded code execution uncertainties such as discretization and convergence issues.

As shown in Fig. 4, the reliability assessment process synthesizes the results of the code execution process through response surface (RS) modelling, subject to an RS fit uncertainty, as well as arc jet test reproducibility and validation uncertainties, failure mode data and modeling uncertainties.

## 2. THE CHALLENGES

### 2.1 Arc Jet Testing

Arc jet testing is the primary means of obtaining data to develop and calibrate the computational models used in ablation prediction; a simplified, one-dimensional sketch of an arc jet test is shown in Fig. 5. In arc jet testing, a TPS sample is exposed to a constant pressure, high heat flux plasma stream for time durations of up to several minutes. Both convective and radiative heat transfer modes are present, but the effects of radiative heat transfer have been ignored within this analysis. The high heat flux flow quickly increases the surface temperature of the material. Thermal conductivity then causes the temperature at all points inside the material to increase, as well. Typically, thermocouples are embedded within the material to measure the thermal response as functions of material depth and time. The effect of uncertainty in the thermocouple (TC) placement, relative to their assumed positions in the material, has not been assessed. When testing ablative materials, the exposure process causes material on the surface to ablate away and the surface undergoes recession. Enthalpy effects are also present within the arc jet flow. Other phenomena occur such as pyrolysis and gas convection through the material. Key material properties known to change during the test, such as density and thermal conductivity cannot be measured during the test. Temperature at bondline, where the TPS is joined by adhesive to the underlying carrier structure, continues to increase well beyond the duration of the test.

A more realistic depiction of arc jet testing is shown in Fig. 6 in which an uneven recession process is illustrated. However, the most common state of practice, and that used currently by this team, is to assume the modelling of the flow is still one-dimensional. True atmospheric re-entry situation for the TPS is even more complicated than shown in Fig. 6 since the flow is neither steady nor one-dimensional.

One specific failure mode is considered within this work; this failure mode occurs when the bondline temperature exceeds the carrier structure allowable temperature. One must attempt to infer the maximum

bondline temperature for the flight TPS based upon the test-anchored computations in order to establish the TPS reliability. There is considerable uncertainty in the arc jet testing and data acquisition process. The uncertainty is quantified, assuming normal distributions, via the non-dimensional statistical form known as the coefficient of variation (COV, given in percent, Eq. 1), which is the standard deviation (StDev) of an uncertainty distribution, divided by the mean value (MV) of the distribution.

$$COV\% = \frac{StDev}{MV} * 100 \quad (1)$$

Test reproducibility uncertainty of bondline thermocouple peak temperatures (comparison of test against test at the same conditions in the same facility) for the TPS under consideration yields COV values of 7% (average) to 38% (maximum), among 12 different samples for the deepest embedded TC sensors, when the mean value and standard deviation are in degrees Rankine. Test validation uncertainty of bondline thermocouple peak temperatures (comparison of test against computation at the same conditions) for the TPS under consideration yields COV measures of 8% (average) to 45% (maximum), among the 24 different samples for the deepest embedded TC sensors.

### 2.2 Generic Data Issues

The overall goal of this work is achieve very high reliability with a quantifiable confidence level for the TPS and failure mode under consideration; for example, a target goal might be stated as to achieve 99% reliability with 95% confidence. Data issues arise in this context simply by the necessary consideration of information in the tails of a given uncertainty distribution. The target reliability statement implies the consideration of data values at two or more standard deviations above the mean value of a given distribution. As shown in Fig. 7, other significant data issues include: *bias, model form, dispersion and sampling uncertainties (descriptions of each follow)*. Unfortunately, these four types of data issues are frequently confounded, and in too many instances, are ignored completely. This paper makes an attempt to identify and quantify these effects for the problem of interest as defined by the following:

*Bias uncertainty* is a shift in the mean value behavior away from the true, but unknown, mean value behavior for the property being sampled. This type of uncertainty is typically associated with testing techniques and is difficult to identify and account for unless tests are conducted in multiple facilities or by differing techniques.

**Model form uncertainty** is the intentional or unknowing use of an incorrect mathematical form to describe the behavior being measured. This type of uncertainty arises because the true model form of the behavior of interest is unknown. Empirical or RS modeling techniques are used to develop a modeling form for the behavior of interest, but one might attempt to model truly cubic behavior with a quadratic model form. This type of uncertainty might be identified by using data from different sources or by employing a robust suite of data modeling options and noting where the prediction discrepancies are important.

**Dispersion uncertainty** is the use of an approximate dispersion model for the behavior of interest, because the true dispersion behavior is unknown. The uncertainty might manifest itself by the use of a wrong distribution type or the by the use of wrong distribution parameters (mean value, standard deviation, skewness and kurtosis). This type of uncertainty might be identified again by using data from different sources or by employing a robust suite of uncertainty modeling options and noting where the prediction discrepancies are important.

**Sampling uncertainty** arises through the use of statistically small sample sets. This type of uncertainty is always present to some extent in most data sets because true statistical convergence of the mean value and standard deviation of a distribution demands million, if not billions, of samples. This type of uncertainty can be overcome to some extent through the use of k-factors applied to the standard deviation or through A- and B-Basis type knockdown factors [7].

For the problem of interest, where small data sample sets are the norm, sampling uncertainties may amount 8% (average) to 24% (maximum) of the mean value and 5% (average) to 15% (maximum) for the standard deviation when considering sets of 100 samples. The sampling uncertainties may amount to 2% (average) to 7% (maximum) of the mean value and 3% (average) to 5% (maximum) for the standard deviation when considering sets of 1000 samples. Even for data sets as large as one million samples, the sampling uncertainties may amount tenths of a percent for both the mean value and standard deviation. This magnitude of uncertainty, by itself, would preclude fulfilling the target reliability statement.

The true cost of sampling convergence is usually prohibitive. Thus, many engineers and project managers are frequently interested in alternative means to state the confidence they have in their data. One such alternative means is the conventional wisdom that one needs at least ten times as many samples as the expected probability of failure. Thus, if the expected probability of failure is 10% (1 in 10 failures, or 90%

reliability), that means 100 samples are needed; if the expected probability of failure is 5% (1 in 20 failures, or 95% reliability), that 200 samples are needed; and if the expected probability of failure is 1% (1 in 100 failures, or 99% reliability), that 1000 samples are needed. Still for many applications, this again requires a prohibitive number of samples.

In order to determine the true minimum number of samples required to achieve a given confidence level, another means is now proposed. This method, the Practical Confidence Limit (PCL), is based upon the statistical underpinnings of the ANalysis Of VAriance (ANOVA) technique employed within this work. The reader is warned that this PCL is a heuristic approach, proposed to define the confidence level of a given set of data, and is independent from explicit consideration of the dispersion of the data set. The PCL will yield the bare minimum number of data samples that could ever be construed as achieving a given confidence level.

To compute the PCL, one must define the minimum number of samples,  $N_{min}$ , required to construct an RS of a given polynomial order (linear, quadratic, etc.) for a given number of independent variables or factors. This minimum number of samples is defined by constructing a D-Optimal Design of Experiment (DOE) [8, 9] for the given number of factors and the given polynomial order (Norder). That minimum number of samples, equal to the number of coefficients needing to be evaluated, will define a unique RS model. One more sample ( $N_{min}+1$ , or  $N_{min}1$ ) is then required to also evaluate the standard deviation of the uncertainty function. This minimum number of samples is then compared with number of samples currently available,  $N$ , to determine the PCL. It is recommended that the number of outlier data points ( $N_{out}$ ), as defined by rigorous statistical tests, be excluded from the comparison, since they do not contribute in a meaningful way to definition of a credible RS. Thus, the PCL is defined as shown in Eq. 2

$$PCL\% = \frac{(N - N_{min}1 - N_{out})}{N} * 100 \quad (2)$$

Thus, to achieve a PCL of 95% for a two parameter RS (MV and StDev, with  $N_{min}1 = 2$ ) would require 40 samples. To achieve a PCL of 99% for a three parameter RS (linear model in one factor, plus a StDev, with  $N_{min}1 = 3$ ) would require 300 samples. The reader will note the small number of samples required compared to the other approaches; moreover, this approach is applicable for any definable RS form. Table 1 provides the values of  $N_{min}1$  for various polynomial orders of RS and various numbers of factors. A linear model is considered when  $N_{order} = 1$ ,

a quadratic when  $N_{order} = 2$ , etc. A two-factor interacting (2FI) DOE, in which the cross linear terms are included but no higher order terms (quadratic, cubic, etc.) is considered when  $N_{order} = 1.5$ ; by definition, no such model (2FI) is possible if  $N_{fact} = 1$  since there is only one factor being considered. For any RS model consisting of simply a mean value and standard deviation,  $N_{min1} = 2$ .

**Table 1. Values of  $N_{min1}$  as a function of the polynomial order and number of DOE factors.**

Norder	Nfact=1	Nfact=2	Nfact=3	Nfact=4	Nfact=5
1	3	4	5	6	7
1.5		5	8	12	17
2	4	7	11	16	22
3	5	11	21	36	57
4	6	16	36	71	127
5	7	22	57	127	253
6	8	29	85	211	463

### 2.3 Material Property Effects / Correlations

The problem of interest for TPS depends upon 11 material property characteristics which are input to the physics-based ablation code:

- virgin density of the material (RHOV)
- char density (RHOC)
- virgin thermal conductivity (XKVRG)
- char thermal conductivity (XKCHR)
- virgin specific heat (CPVRG)
- char specific heat (CPCHR)
- virgin emittance (EMVT)
- char emittance (EMCT)
- normalized recession parameter (ZBPRIM, otherwise known as the B' tables)
- roughness height (ROUGHT)
- pyrolysis gas enthalpy (CPGAS).

Some of these parameters are measured, other are treated as tuning constants in an attempt to calibrate the computations to best match arc jet test results. Testing for some of these parameters is quite challenging due to the environments required (arc jet flows); multiple testing techniques may be used for some of the material properties. In the present work, a complicated situation results that employs data from multiple testing sources. Large bias uncertainties are present for several variables. Different data sets also used to

define mean value and dispersion behaviors. The accepted values of the material property COV are provided in Table 2. However, additional sampling uncertainties associated with the mean value and standard deviations of the variables, on average 52% and 35%, respectively, may be appropriate to consider.

**Table 2. Accepted COV values for the 11 material property input variables.**

Variable	COV%
RHOV	4
RHOC	4
CPVRG	5
CPCHR	10
XKVRG	7.5
XKCHR	25
EMCT	2
EMVT	5
ROUGHT	25
ZBPRIM	20
CPGAS	25

An additional concern related to these material property variables occurs when the uncertainty of a single material property variable simultaneously increases both the recession amount and bondline temperature. Since increased recession would bring the high heat flux flow closer to the bondline, this synergistic combination of uncertainty effects can potentially lead to a significant under prediction of the bondline temperature. This effect does occur (up to 13% of the bondline temperature in degrees Rankine) for several of the key material property variables including RHOV, CHCPR, EMCT, ROUGHT and CPGAS for the data examined.

Another material property effect of concern occurs when the correlation of two distinct material property uncertainties simultaneously increases the recession amount and bondline temperature. This synergistic combination of uncertainty correlation effects occurs in several correlation combinations anticipated by the SME team; specially, this situation occurs (up to 20% of the bondline temperature in degrees Rankine) for correlations between RHOV and RHOC, RHOV and CVPRG, RHOV and CPCHR, RHOV and XKVRG, RHOV and CPGAS, RHOC and ROUGHT, and for RHOC and ZBPRIM. Data bias is also observed in the measurements for XKVRG (18%), thermal diffusivity (15%), CPVRG (14%) and EMCT (2%) for the data examined. These effects are not explicitly considered in the present formulation.

## 2.4 Trajectory/ Orientation

Uncertainties in the vehicle trajectory during atmospheric re-entry may also be significant, due to uncertainties in the atmospheric conditions (e.g., pressure, density, viscosity) that are experienced. Each body point of the heat shield experiences a unique combination of pressures and heat fluxes. As shown in Fig. 8, seven body points were selected for analysis to represent the different TPS sizing regions of the heat shield. The colors in Fig. 8 are intended to notionally suggest hotter (red) and cooler (blue) surface temperature regions of the TPS. The differences experienced by the various body points for a given mission are considerable: a COV of about 100% in recession amount and a COV of about 3% to 11% in bondline temperature at specific body points have been observed. The situation is exacerbated when the heat shield is designed to service more than one mission. In this situation, COV increments from one mission to another were observed as large as 86% in recession and about 40% in bondline temperature.

## 2.5 Transitional Flow

Other effects, such as an uncertain transition front from laminar to turbulent flow may significantly affect the heat transfer to the TPS. This effect only occurred for one of the body points studied. The uncertainty due to plausible material property variations, coupled with the presence of transitional flow, was found to represent a significant increment in both the predicted bondline temperature and recession. It is quite possible that the a-priori choice of the seven body points does not actually identify where the worst conditions occur as a result of flow transition. One attempt to identify where the worst conditions might occur as a result of flow transition was undertaken and resulted in a small increment (few percent) to the bondline temperature and a larger increment (maybe 20%) in the recession.

Standard TPS design practice is to assume the trajectory uncertainties from mission to mission and from body point to body point are covered by design margin/space assumptions (factors of safety, typically 10% to 15%) applied to the anticipated pressure and heat flux. However, these factors of safety provide no insight into the true TPS reliability and may even provide a false sense of security that TPS is very reliable when it is not. Furthermore, this work suggests that the established margining assumptions may not adequately cover the identified and quantifiable uncertainties within the process, especially when transitional flow is present.

## 2.6 Ground-to-Flight Uncertainty

Ground-to-flight uncertainty is the uncertainty due to TPS testing and development in incorrect aerothermal environments, namely ground-based facilities that cannot duplicate the three-dimensional continuously varying conditions of atmospheric re-entry. It is expected that using margining assumptions will cover all ground to flight corrections. As this aspect of the work was not explicitly addressed within the scope of research performed in writing this paper, a literature survey was undertaken to identify ground-to-flight corrections that others have used [10-13]. In particular, stagnation pressure corrections of 18% were identified by two references, and uncertainties in the heat flux of 13% to 69% were also found. A code comparison conducted by the Thermal Performance Database Team yielded thermocouple differences up to 25%. Other findings of note were uncertainties in the char thickness of up to 42% and uncertainties in the axial force coefficient of about 6%, which directly influences the ballistic coefficient of the vehicle. An investigation of Project Mercury (1961 through 1963) revealed potential bondline temperature uncertainties on the order of several hundred degrees [14] which is comparable to the current situation. The Apollo capsules (1968 through 1972) were designed with considerable margin (see Figure 10 in [15]); Apollo 4 was closest to the design limit. This suggests that there has been little advancement in the past 50 years in understanding the many critical TPS uncertainties.

## 2.7 Failure Mode Form

This bondline over temperature failure mode is illustrated in Fig. 9. Because the exact TPS failure conditions are unknown, a model is used to predict failure in which the probability of TPS failure increases from zero to unity as the bondline temperature increases above some safe temperature. However, the temperature used to determine the probability of failure is subject to numerous uncertainties, as have already been noted, and thus is really a distribution with a mean value and a standard deviation. Also, the exact form of the failure mode is not known and so there may be an optimistic representation of the failure mode (solid line in Fig. 9), as well as a pessimistic representation of the failure mode (dashed line in Fig. 9); the pessimistic version yields high probabilities of TPS failure for a given temperature just above the safe temperature. The difference between the two versions of the TPS failure probability ( $\Delta P_{fail}$ ) has been found to be a significant contributor to the reliability assessment because just a small change in the failure probability (or conversely, the reliability estimate, which is  $Rel = 1 - P_{fail}$ ) can easily make the difference

between a fully reliable TPS and one that fails to meet the target reliability.

## 2.8 Reliability Assessment

A physics-based probabilistic reliability assessment process is assembled and executed. Each of the uncertainties identified along the path are modeled appropriately. A choice must be made as to how to solve the probabilistic reliability assessment problem. Typical choices for this are the Monte Carlo Simulation (MCS) and First-Order Reliability Method (FORM). The advantage of MCS is that is easy to implement and execute; however, without a very large number of samples, the method is not suitable for very high reliability assessments because of the extremely slow convergence of properties in the tails of a distribution [16]. Millions or billions of physics-based model solutions may be required to adequately converge the statistical results far away from the mean value (i.e., the tails of a distribution) to a high confidence level, depending upon the amount of dispersion present. Other simulation variants also exist including Latin Hypercube and directional methods which may require significantly fewer samples to achieve comparable convergence levels. The advantage of FORM is that it may require significantly fewer physics-based model solutions; however, this approach is not as robust as MCS and generally requires SME oversight.

Other effects come strongly into consideration at this point, as well. As shown in Fig. 10, the achievable reliability is a distribution expected to lie above the required or target reliability; this can be easily achieved if the required reliability is quite low, such as 50%. But, the reliability for mission critical and human critical systems, such as the TPS, with no redundancy, is typically required to be in excess of 99%. Thus, the reliability distribution gets squeezed into a small very small window and less tolerance exists for uncertainty in the reliability estimate as the required reliability approaches 100% (see Fig. 11).

## 2.9 Reliability Cascade

This requirement to achieve very high reliability with very little tolerance for uncertainty also propagates backward through the system analysis. Moreover, as several independent subsystem failure modes feed the system failure mode, the required reliability is found to be even higher for the subsystems than for the system. If the required reliability for the system is defined by  $RSYS$ , and there are  $M$  independent subsystems feeding the system failure mode, the required reliability for each of the subsystems,  $RSUB$ , is given by the expression

$$RSUB = RSYS^{1/M} \quad (3)$$

Thus, if the subsystem reliability for each of two independent subsystems is 90%, the system reliability is only 81%; conversely, if the required reliability is 90% for a system with three independent subsystems, each subsystem must achieve a reliability of almost 97%.

## 2.10 Cost-Benefit Modeling

The final challenge, and perhaps the most difficult to address in a programmatic sense (so far as achieving an overall high confidence level), is that of cost-benefit modeling. This challenge must be overcome if one is to improve upon the estimated reliability that is computed based upon the elements of the previous discussion. Each aforementioned uncertainty presents a unique investment opportunity. Each uncertainty has specific means to reduce the uncertainty and specific costs and benefits associated with it as a potential investment. In order to make the best specific investment recommendations, one must fairly and consistently evaluate the cost and potential benefit of each investment option. The challenge for this item lies in achieving a very high degree of concurrence among the various technical and managerial stakeholders that the required cost-benefit modeling is not only credible but sufficiently correct to enable defining valid investment recommendations.

A sample Bayesian cost-benefit analysis is shown in Fig. 12. This process attempts to answer four questions: 1) what is the unit of purchase and what does a unit of purchase cost, 2) how many units of purchase are needed, 3) how much will a unit of purchase influence the outcome, and 4) why should one invest in this option over another choice? The answers to these questions inform the cost-benefit modeling process.

The investment opportunities include obtaining new testing results, new testing and measurement capabilities and improved computational methods that can be brought to bear upon the uncertainty issues. Some issues, such as the failure mode modeling might be best addressed by convening an SME panel to discuss the possible options. It is important to realize that the means by which one might reduce one uncertainty are very likely quite different from those that might address a second uncertainty, as are the costs and benefits.

All of the above information is assembled together into a physics-based probabilistic reliability assessment process. Each of the uncertainties identified along the path must be modelled appropriately (credible

distribution type and distribution parameters). In this work, many of the uncertainties are simply modelled as normal distributions, though other distributions could and should be investigated to determine the robustness of the reliability estimate. The primary outputs of the probabilistic reliability assessment process are threefold: 1) the mean value reliability estimate, 2) the reliability estimate distribution value at 95% confidence, and 3) the reliability estimate sensitivities to the modelled uncertainties (both mean value and standard deviation sensitivities). The first two of these three outputs are used to determine if the TPS meets the target reliability statement. The third output is used to inform other subsequent analyses, such as a resource allocation process and a design under uncertainty process.

A resource allocation process was developed from this TPS reliability assessment in order to make specific recommendations about where best to invest resources among numerous potential investment options in order to improve one or more of the following benefit metrics: 1) the mean value reliability estimate, 2) the reliability distribution standard deviation, and/or 3) the confidence level associated with the mean value reliability estimate and its standard deviation. At the heart of the resource allocation process is a cost / benefit modeling and assessment process. The chain rule must be invoked to correctly define the investment merit:

$$Benefit\ Merit = \frac{\partial Benefit}{\partial X} * \frac{\partial X}{\partial Unit} * Nunits \quad (4)$$

$$Cost\ Merit = \frac{\partial Cost}{\partial Unit} * Nunits \quad (5)$$

$$Investment\ Merit = \frac{Benefit\ Merit}{Cost\ Merit} \quad (6)$$

For each potential investment option, X (typically, an uncertainty MV or StDev), a unit of purchase was defined. The number of units (Nunits) helps to define both the benefit and cost. The first term in the right hand side of Eq. 4 is the probabilistic, physics-based sensitivity. The second term in Eq. 4 is the most problematic; this term translates a change a MV or StDev of an uncertainty into units of purchase. This is not well defined and may be highly subjective.

For many options, the unit of purchase was simply a test (either an arc jet or materials property test); the cost of a unit of purchase could be determined by SME polling. However, some units of purchase are much more difficult to define; for example, to improve the test reproducibility uncertainty, one could invest in better arc jet testing or measurement methods and to improve the test validation uncertainty, one could

invest in improvements to the basic computational ablation model. To improve the failure mode definition, one might need to invest in hours of programmatic discussion to help better define, and achieve consensus, on the failure mode(s) of interest.

It is critical that a credible model of the cost and benefit be developed for each investment option being considered. Then, having defined credible cost / benefit models for each of the possible investment options, the individual pieces are assembled together in a system resource allocation Bayesian network model; a sample resource allocation Bayesian network for eight investment options is notionally shown in Fig. 13, with one investment option leg highlighted in red. The goal of this figure is simply to illustrate the level of modeling complexity involved in solving the resource allocation problem. The central cyan colored node, "Where to Invest?" is the heart of the resource allocation problem. The eight nodes immediately surrounding this central node (yellow, purple, orange and red) are the possible investment options. Each of the cyan nodes connected to the investment option nodes asks one of the questions "Is Benefit Merit High" and "Is Cost Merit High?" (i.e., meaning low cost); each of these questions is then broken down further, as shown in Fig. 12, to aid in SME evaluation of the investment options. A favorable investment merit, as defined by Eq. 6, means large "bang for the buck".

The probabilistic reliability assessment process sensitivities are used to properly scale the investment merit of each option. This network, when interpreted correctly, then allows one to determine specific recommendations for investment ranking. Such has been done within the scope of this work by using a combination of SME cost / benefit assessments and physical sensitivities.

The results of a similar effort for 19 possible investment options, subject to many assumption and caveats, indicate the most fruitful investment areas are computational improvements, arc jet testing improvements, more arc jet reproducibility and validation test samples, and more failure mode test samples. These are the areas of the greatest uncertainty and influence within the reliability assessment.

An uncertainty design process has likewise been developed and executed based upon the probabilistic reliability assessment process sensitivities. In this process, the analyst changes the TPS thickness in the presence of all the other quantified uncertainties. This process allows one to determine the TPS thickness for each of the seven body points under consideration, for

the current vehicle trajectory, such that the TPS meets the target reliability statement.

### 3. SUMMARY

Numerous uncertainties for a human-rated TPS system have been identified and quantified. Among the greatest challenges are improving the reproducibility and validation of the arc jet test results, properly statistical convergence of data, material property correlations, the effects of flow transition upon the chosen failure mode, the effects of a reliability cascade backward through the process and credible cost / benefit modeling to enable improving upon the current situation. The various uncertainties have been modelled within a physics-based probabilistic reliability assessment process and propagated through the process to determine a TPS reliability estimate distribution and its sensitivities to both the mean value and standard of the modelled uncertainties. The sensitivities are then used to drive both resource allocation and design under uncertainty processes.

### REFERENCES

1. *Standard for Models and Simulations*, NASA-STD-7009, 2008.
2. Blattnig, S. R., Luckring, J. M., Morrison, J. H., Sylvester, A. J., Tripathi, R. K. and Zang, T. A. NASA Standard for Models and Simulations: Philosophy and Requirements Overview, AIAA 2009-1010, 2009.
3. Green, L. L., Blattnig, S. R., Luckring, J. M. and Tripathi, R.: "An Uncertainty Structure Matrix for Models and Simulations." AIAA 2008-2154, 2008.
4. Guidance for Space Program Modeling and Simulation, The Aerospace Corporation Report Number TOR-2010(8591)-17, 2010.
5. Vander Kam, J. C., Howard, A. R., Gage, P., Schiermeier, J. E., The Devil's in the Tails – Reliability Prediction Methodologies for the Orion Heat Shield, AIAA 2011-422, 2011.
6. Cozmuta, I., Wright, M. J., Laub, B., Willcockson, W. H., Defining Ablative Thermal Protection System Margins for Planetary Entry Vehicles, AIAA 2011-3757, 2011.
7. Department of Defense Handbook: Polymer Matrix Composites Guidelines for Characterization of Structural Materials, MIL-HDBK-17-1E.
8. Giunta, A. A., Narducci, R., Burgee, S., Grossman, B., Haftka, R.T., Mason, W.H., and Watson, L.T., "Variable-Complexity Response Surface Aerodynamic Design of an HSCT Wing." Proceedings of the 13th AIAA Applied Aerodynamics Conference, San Diego, CA / June 19-22, 1995, pp. 994-1002.( AIAA 95-1886 ).
9. D-Optimal designs website, Engineering Statistics Handbook, <http://www.itl.nist.gov/div898/handbook/pri/section5/pri521.htm> (accessed 5/14/2013).
10. Subrahmanyam, P., Papadopoulos, P., Trajectory Based Computational Aerothermodynamic Investigation Tool SPARTA for Planetary Entry Probes, Department of Mechanical and Aerospace Engineering, Center of Excellence for Space Transportation & Exploration, San Jose State University, One Washington Square, San Jose, CA. 95192, USA. prasub@gmail.com, ppapado1@email.sjsu.edu.
11. Overview of Intercalibration Results A Model Comparison. 4th Ablator Modeling Workshop, Albuquerque, NM, March 1st-3rd, Thermal Performance Database Team, March 3, 2011.
12. Mahzari, M., Braun, R. D. and White, T. R., Reconstruction of Mars Pathfinder Aerothermal Heating and Heatshield Material Response Using Inverse Methods AIAA 2012=2872, 2012.
13. Murray, A., Coupled Aeroheating / Ablation Analysis for Re-Entry Vehicles, ITT Aerotherm, 6767 Old Madison Pike, Ste 310, Huntsville, AL 35806, 256-964-1474, [al.murray@itt.com](mailto:al.murray@itt.com).
14. Capsule Systems - Thermal Control Systems, <http://www.angelfire.com/space2/sp425/23.html> (accessed 5/14/2013).
15. Pavlosky, J. E. and St. Leger, L. G., Apollo Experience Report – Thermal Protection Subsystem, NASA TN D-7564.
16. Haldar, A. and Mahadevan, S., *Probability, Reliability, and Statistical Methods in Engineering Design*, ISBN: 978-0-471-33119-3, Copyright © 2000-2013 by John Wiley & Sons, Inc.

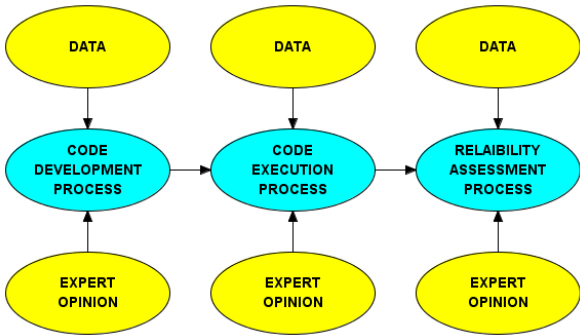


Fig. 1. Generic synthesis and modeling process.

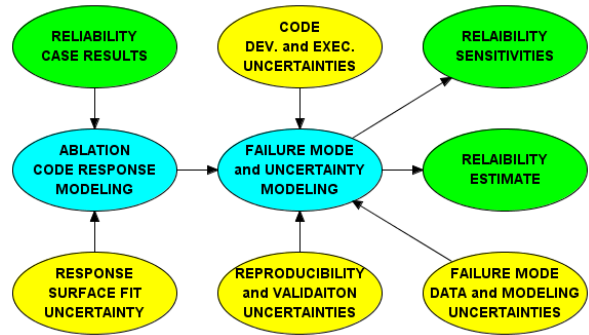


Fig. 4. Generic reliability assessment process.

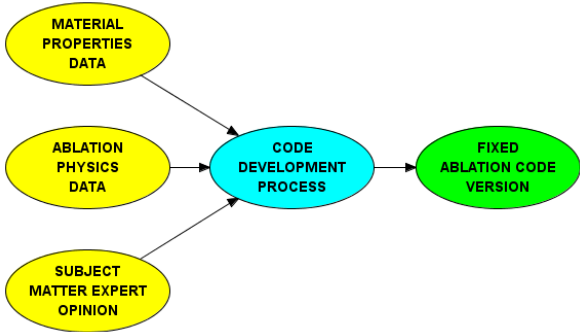


Fig. 2. Generic code development process.

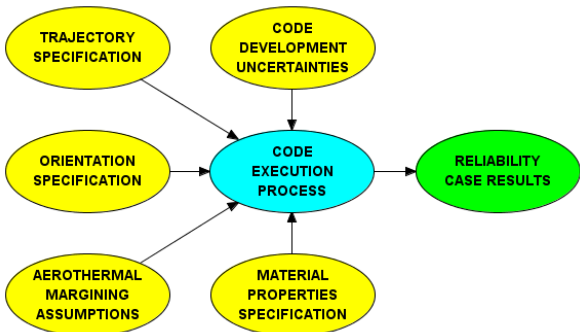


Fig. 3. Generic code execution process.

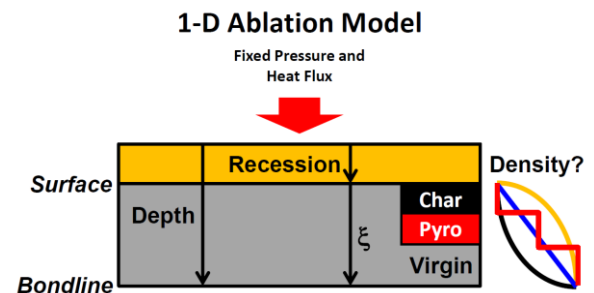


Fig. 5. One-Dimensional ablation process.

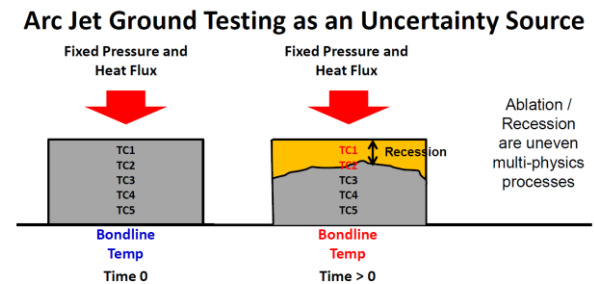


Fig. 6. Arc jet testing process sketch.

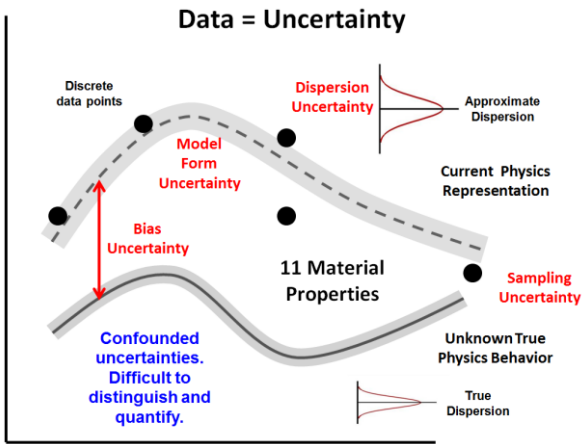


Fig. 7 Uncertainties sketch.

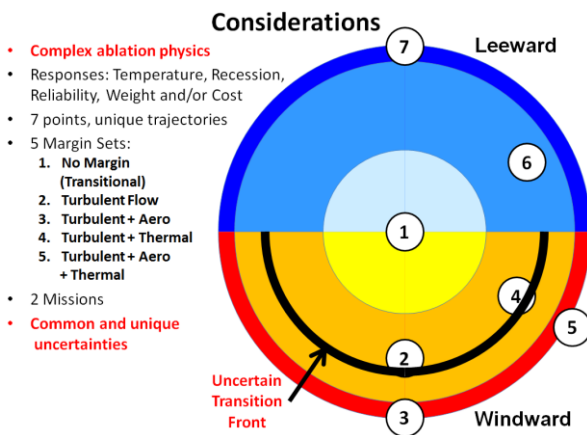


Fig. 8. Heat shield body points sketch.

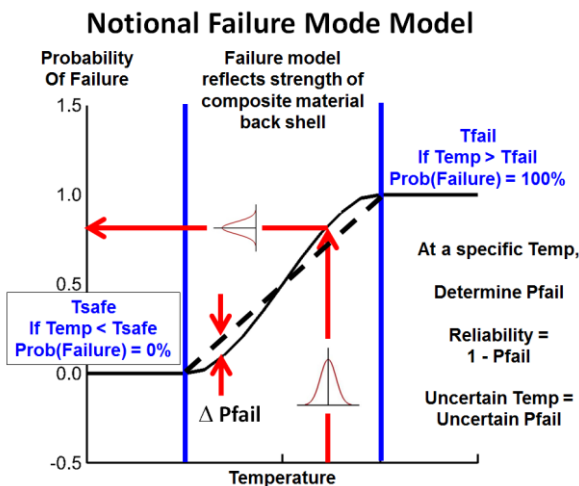


Fig. 9. Failure mode sketch.

### Reliability Estimation

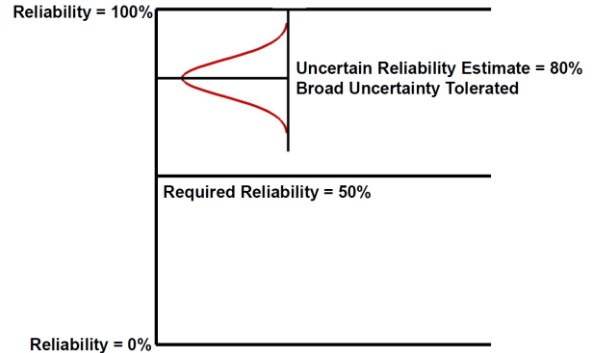


Fig. 10. Reliability estimation sketch, required reliability = 50% .

### Reliability Estimation

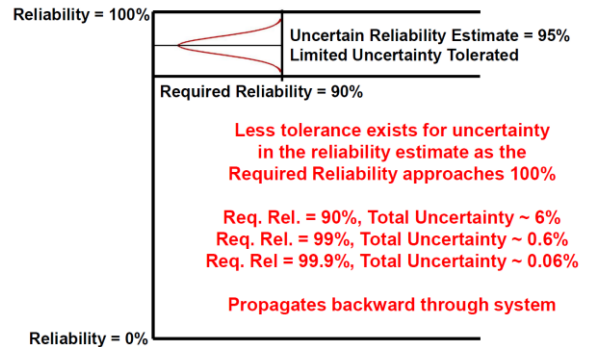


Fig. 11. Reliability estimation sketch, required reliability = 90% .

### Generic Cost to Benefit Ratio Evaluation

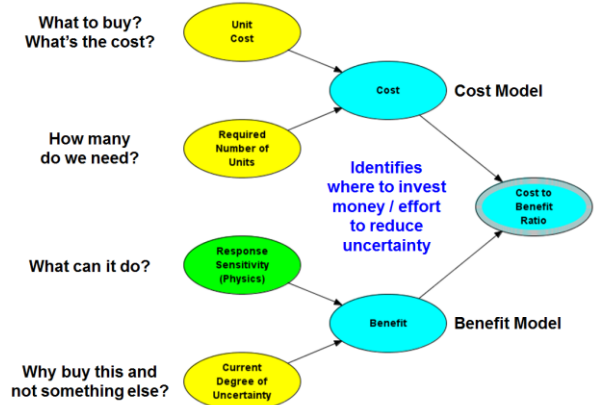


Fig. 12. Generic cost / benefit modeling Bayesian network sketch.

# 8-Factor Resource Allocation Process

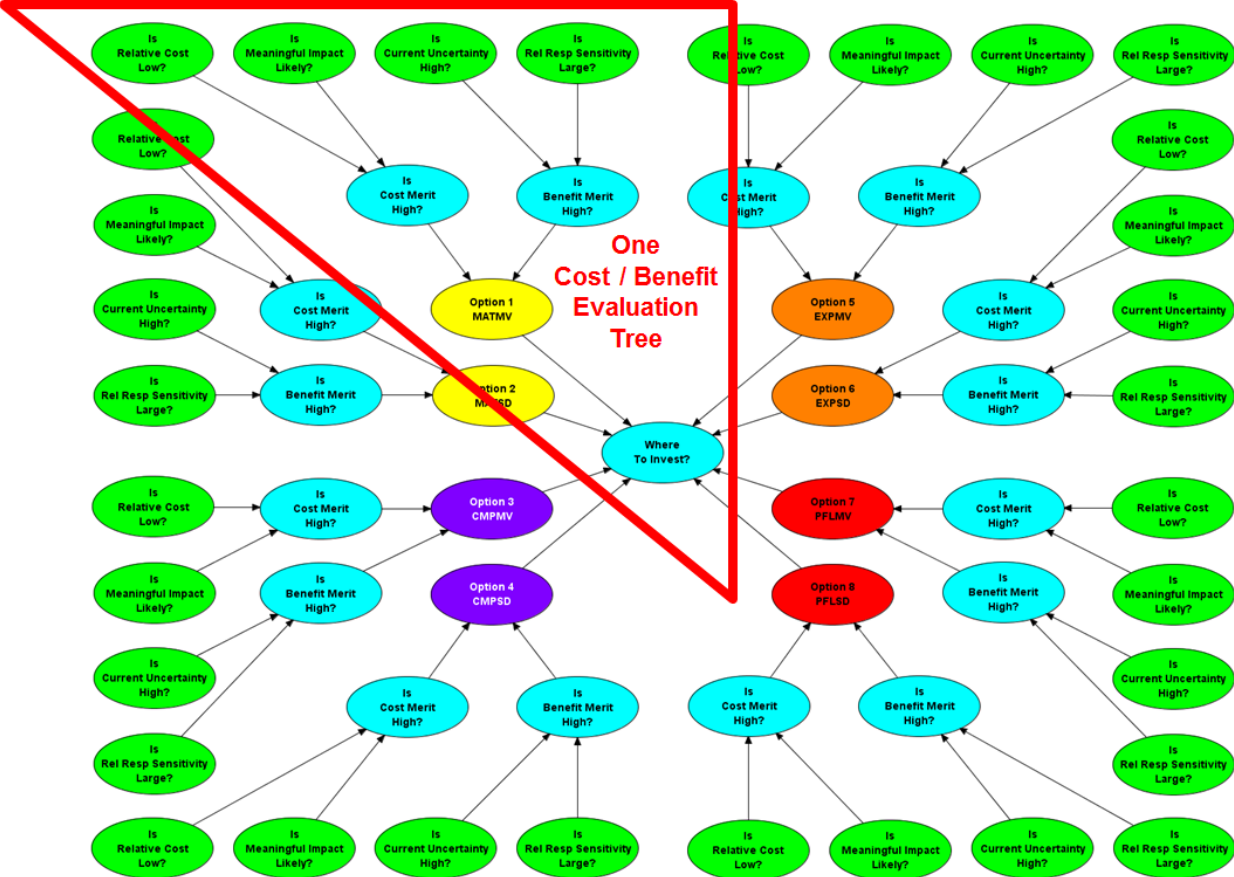


Fig. 13. Generic 8-option resource allocation Bayesian network sketch.